Limited mitochondrial capacity of visceral versus subcutaneous white adipocytes in male C57BL/6N mice

Theresa Schöttl, Lisa Kappler, Katharina Braun, Tobias Fromme, Martin Klingenspor*

Molecular Nutritional Medicine, Technische Universität München, Else Kröner Fresenius Center for Nutritional Medicine, Freising, Germany

Accumulation of visceral fat is associated with metabolic risk whereas excessive amounts of peripheral fat are considered less problematic. At the same time, altered white adipocyte mitochondrial bioenergetics has been implicated in the pathogenesis of insulin resistance and type 2 diabetes. We therefore investigated whether the metabolic risk of visceral versus peripheral fat coincides with a difference in mitochondrial capacity of white adipocytes.

We assessed bioenergetic parameters of subcutaneous inguinal and visceral epididymal white adipocytes from male C57BL/6N mice employing a comprehensive respirometry setup of intact and permeabilized adipocytes as well as isolated mitochondria. Inguinal adipocytes clearly featured a higher respiratory capacity attributable to increased mitochondrial respiratory chain content as compared to epididymal adipocytes. The lower capacity of mitochondria from epididymal adipocytes was accompanied by an increased generation of reactive oxygen species per oxygen consumed. Feeding a high-fat diet for one week reduced white adipocyte mitochondrial capacity, with stronger effects in epididymal when compared to inguinal adipocytes. This was accompanied by impaired body glucose homeostasis. Therefore, the limited bioenergetic performance combined with the proportionally higher generation of reactive oxygen species of visceral adipocytes could be seen as a candidate mechanism mediating the elevated metabolic risk associated with this fat depot.

Obesity is a well-known risk factor for numerous pathologies including insulin resistance, type 2 diabetes, hypertension and dyslipidemia, together forming the core of the metabolic syndrome (1–3). Although obesity in general is defined as an excess of body fat, not all adipose tissue depots seem to contribute to this increased risk to the same extent. Already in 1956, Jean Vagues pioneering work indicated a phenomenon later confirmed in multiple ways: While even large amounts of subcutaneous fat mass are unproblematic for metabolic health, extensive visceral fat is an established risk factor for insulin resistance and type 2 diabetes (4–8). Intra-abdominal transplantation of subcutaneous fat even ameliorates metabolic health, whereas transplantation of visceral fat does not (6, 7).

These fascinating observations led to intense research aiming to elucidate the underlying mechanisms (9–13). Comparisons on the level of cell physiology revealed a wide range of differences between the anatomically distinct white adipose tissues (14). To only name a few, stimulated lipolysis is higher in visceral than in subcutaneous fat (15, 16), the expression pattern of adipokines differs (17–19) and of note, it has been proposed that subcutaneous and visceral adipocytes have a different developmental origin (20). Thus, in contrast to the opposing view of adipose tissue forming a single organ with a multidepot organization (21–23), it has been suggested that each single fat depot should be regarded a separate mini-organ (20).

ISSN Print 0013-7227 ISSN Online 1945-7170
Printed in U.S.A.

Received August 14, 2014. Accepted December 22, 2014.

Abbreviations: CS citrate synthase, cRCR cellular respiratory control ratio, faf fatty acid free, FCCP carbonyl cyanide 4-(trifluoromethoxy) phenylhydrazone, HSP60 mitochondrial heat shock protein 60, mtDNA mitochondrial DNA, nDNA nuclear DNA, OXPHOS oxidative phosphorylation, RCR respiratory control ratio, SOD2 superoxide dismutase 2

Importantly, studies in both mice and men uncovered a correlation between impaired white adipocyte mitochondrial function and the deranged glucose homeostasis accompanying obesity (24–29). However, these data are mainly based on surrogate measures like mitochondrial DNA abundance, mitochondrial mRNA and protein levels, electron microscopy (EM) or citrate synthase activity measurements. State of the art functional analyses of white adipocyte mitochondrial bioenergetics are rather scarce in this context. Additionally, often only a single depot is investigated and extrapolated to the entirety of body fat.

In this study, we characterized mitochondrial bioenergetics of murine subcutaneous inguinal and visceral epididymal white adipocytes with an unprecedented array of state-of-the-art methodology including respirometry of intact and permeabilized adipocytes as well as isolated mitochondria. We specifically isolated mature white adipocytes to exclude all effects of other celltypes resident in adipose tissue. We here demonstrate a higher respiratory capacity of inguinal as compared to epididymal adipocytes. This finding holds true on the level of intact adipocytes, permeabilized adipocytes and isolated mitochondria.

In a next step we analyzed mitochondrial function of both types of adipocytes after high-fat diet feeding for one week. This resulted in a reduction of white adipocyte mitochondrial capacity. Of note, the limitation was more pronounced in epididymal when compared to inguinal adipocytes and was accompanied by impaired whole body glucose homeostasis. Thus, the limited bioenergetic capacity of adipocytes from visceral fat may be part of the elevated metabolic risk associated with this fat depot.

Materials and Methods

Mice

General. Experiments were performed on 12 weeks old male wildtype C57BL/6N mice (Charles River) which were housed in groups in a specific pathogen-free environment on a 12:12h light-dark photocycle at 22°C with ad libitum access to water and food (CHOW, type M-Z, Ssniff; Soest, Germany). This study is in accordance with the German animal welfare law and with permission of the government of Upper Bavaria (Regierung von Oberbayern, reference number Az. 55.2.1.54–2532–148–13).

High-fat diet feeding. At the age of 7 weeks wildtype C57BL/6N mice were switched from CHOW to a purified research control diet (CD, 12 kJ% fat, SS745-E702, Ssniff). After acclimatization for one week mice were matched by body weight into a control (CD) and a high-fat diet group (HFD, 48 kJ% fat SS745-E712; Ssniff). Feeding was conducted for one week.

Body weight and body composition

Body weight was measured before and after the HFD vs CD feeding trial. Body composition was measured with nuclear magnetic resonance spectroscopy (The Minispec mq 7.5 POY Live mice analyzer, Bruker, Billerica, MA, USA) at the end of the feeding period.

Oral glucose tolerance test

After a fasting period of 6 hours mice received 2.66 mg glucose per [(lean mass + 0.2 fat mass) g] by single oral gavage (30). Blood glucose was monitored before and 15, 30, 60 and 90 minutes after gavage. Total area-underthe-curve (AUC) was calculated as measure for glucose tolerance.

Tissue dissection and isolation of adipocytes

Mice were killed by carbon dioxide exposure and exsanguination. Inguinal (=posterior subcutaneous) and epididymal fat depots were dissected and weighed. Visible blood vessels were removed. For experiments on isolated mitochondria, inguinal and epididymal fat depots from 15 mice were pooled separately and minced into small pieces. For measurements on intact or permeabilized adipocytes, fat depots of individual mice were used.

Mature adipocytes were separated from other cell types by collagenase-digestion (Type A, Roche Applied Science; Penzberg, Germany; 1 g/l in Hank's Balanced Salt Solution [HBSS 14 025–092, Gibco®, live technologies]) containing 4% BSA) at 37°C in a shaking incubator (WiseCube WIS-20, Wisd laboratory instruments, Witeg; Wertheim, Germany, 150 rpm), filtering through a 250 μM nylon gauze and subsequent low spin centrifugation (300*g*, 2 minutes, RT). Floating mature adipocytes were washed twice with STE-buffer containing 4% BSA (250 mM sucrose, 5 mM Tris, 2 mM EGTA, pH = 7.4 at 4°C). Washing steps were repeated two times more with STE containing 4% essentially fatty acid free (faf) BSA. Floating adipocytes were stored in STE on ice until the respective respirometry measurements were performed (not longer than 4h).

Histology

Paraffin embedded adipose tissue samples were sliced into 5 μm sections, mounted and stained with hematoxylin and eosin. Cell diameters were analyzed in fat depots of six mice each with five independent histological sections. Adipocyte size was determined using a macro specifically developed for automated image analysis of adipose tissue (WimAdipose, Wimasis GmbH; Munich, Germany).

Respirometry of adipocytes

Oxygen consumption of adipocytes was measured with high resolution respirometry (Oxygraph-2k, OROBOROS INSTRUMENTS; Innsbruck, Austria). 100 μl of adipocyte suspension was pipetted into 2 ml MIR05 buffer (110 mM sucrose, 60 mM potassium lactobionate, 0.5 mM EGTA, 3 mM $MgCl_2$ * $6H_2O$, 20 mM taurine, 10 mM KH_2PO_4, 20 mM Hepes, 1g/l BSA-faf, for intact cells 5 mM malate, pH 7.1 at 37°C, as described by OROBOROS INSTRUMENTS). The stirrer speed was set to 750 rpm.

For oxygen consumption measurements of intact adipocytes, pyruvate (5 mM) was injected and basal cellular respiration was recorded. Proton leak respiration was assessed by addition of

oligomycin (2 μg/ml). Titration of carbonyl cyanide 4-(trifluoromethoxy) phenylhydrazone (FCCP, 0.5 μM steps) was performed for measuring maximal cellular respiration rates. Nonmitochondrial oxygen consumption determined in the presence of antimycin A (2.5 μM) was subtracted from the other respiratory states. Spare respiratory capacity was calculated by subtracting basal from maximal oxygen consumption rates. For mitochondrial integrity control, cellular respiratory control ratio (cRCR) was calculated as the ratio of maximal to leak oxygen consumption.

For oxygen consumption measurements of permeabilized adipocytes, 2 μM digitonin was added. State 4 respiration was measured in the presence of succinate/rotenone (5 mM/2 μM). By addition of ADP (5 mM) phosphorylating state 3 was induced. ATP synthase was inhibited by oligomycin (2 μg/ml) (state 4o). Titration of FCCP (0.5 μM steps) was performed for measuring maximal cellular respiration rates (state 3u). Nonmitochondrial oxygen consumption determined in presence of antimycin A (2.5 μM) and subtracted from the other respiratory states. Respiratory Control Ratio (RCR) was calculated dividing state 3 by state 4o respiration.

Cellular DNA quantification

DNA content of adipocyte suspensions was quantified by quantitative PCR targeting a unique region of genomic DNA (promotor resistin). Samples were diluted 1:5 in digestion buffer (50 mM KCL, 0.45% Nonidet P-40, 0.45% Tween 20, 0.2 mg/ml Proteinase K) and incubated for 1 hour at 65°C under agitation (1000 rpm). Proteinase K was inactivated at 95°C for 10 minutes and 2.25 volumes phenol:chloroform:isoamyl alcohol (25:24:1, Carl Roth GmbH & Co. KG; Karlsruhe, Germany) were added. After phase separation by centrifugation at 16 000*g* for 10 minutes the hydrophilic phase was used for qPCR (Roche Lightcycler 480 II;Roche; Basel, Switzerland) using a commercial premix (SensiMix no Rox;Bioline; London, Great Britain). Primers (fw 5′-ACCTCTCTTGGGGTCAGATGT-3′, rev 5′-CTGGGTATTAGCTCCTGTCCC-3′) were synthesized by Eurofins MWG Operons. DNA concentrations were determined by comparison with a mouse gDNA standard dilution series of known concentration.

Quantification of mtDNA

DNA was isolated from adipocytes using the Wizard® SV Genomic DNA Purification System (A 2360, Promega, Fitchburg, WI, USA). Yield was quantified spectrophotometrically (TECAN Infinite® M200, NanoQuant, Tecan Group Ltd.). DNA were amplified with specific primers (nuclear: fw 'tttacaggatctccaagattcaga' rw 'gatcaccccatgtgaacaaa'; mitochondrial: fw 'caaatttacccgctactcaactc' rw' gctataatttttcgtatttgtgtttgg'). Quantification of PCR amplification was achieved by specific probes (Universal ProbeLibrary, Roche; nuclear no 26, cat. no. 04687574001; mitochondrial no. 101, cat. no. 04692195001).

Citrate synthase activity

Adipocyte suspensions containing 1% Tween 20 were homogenized (ULTRA-TURRAX, IKA; Staufen, Germany) and diluted 1:25 in reaction buffer (100 mM Tris, 1 mM $MgCl_2$, 1 mM EGTA, 0.1 mM DTNB, 3.6 mM Acetyl-CoA, pH 8.2). Absorption was measured at 30°C and 412 nm with a microplate reader (TECAN Infinite® M200, Tecan Group Ltd.; Männedorf, Switzerland) for 5 minutes before oxaloacetate (0.5 mM) was injected. Data were recorded for 10 minutes. Enzyme activity [μmol/min*mg protein] was calculated on the basis of the absorption change before and after injection of oxaloacetate with respect to dilution factor, extinction coefficient of DTNB and pathlength of the plate.

Isolation of mitochondria

Mitochondria were isolated from mature adipocytes by homogenization and differential centrifugation. All steps were conducted at 4°C or on ice. Adipocytes were transferred into a glass-teflon homogenizer (15 ml), filled with STE to 15 ml and manually disrupted by 5 rotating strokes. The homogenate was transferred to a 40 ml centrifuge tube, filled up with STE-buffer containing 4% BSA-faf and centrifuged for 10 minutes at 800 *g*. Supernatant was transferred to a second tube and centrifuged for 10 minutes at 10 000 *g*, whereas the pellet was homogenized and centrifuged for 10 minutes at 800 *g* once more. Again, the supernatant was transferred to a new centrifuge tube and centrifuged for 10min at 10 000 *g*. Supernatants of both fast-spins were discarded, the pellets were resuspended in KHE-buffer (120 mM KCL, 5 mM KH_2PO_4, 3 mM HEPES, 1 mM EGTA, 0.5% BSA-faf, pH = 7.2) and combined in a single centrifuge tube. The fast spin was repeated. Again, supernatant was discarded and the mitochondrial pellet resuspended in KHE.

Quantification of mitochondrial protein

Protein concentration of mitochondrial suspensions was determined by the Bradford method. Mitochondrial suspensions were diluted 1:200 in Bradford reagent (Roti®-Quant, Carl ROTH; Karlsruhe, Germany; diluted 2:7.5). Absorbance was measured at 590 nm with a microplate reader (TECAN Infinite® M200, Tecan Group Ltd.). Mitochondrial protein concentration was assessed using a KHE-diluted BSA standard.

Respirometry of isolated mitochondria

Mitochondrial respiration was assessed by the XF96 Extracellular Flux Analyzer (Seahorse Bioscience, Billerica, Massachusetts). Sensor cartridges were hydrated overnight in the XF Prep Station at 37°C (Seahorse Bioscience) using the XF96 Calibrant solution (200 μl per well). Isolated mitochondria were seeded in collagen coated XF96-PS cell culture plates (5 μg per well in 20 μl KHE either containing 5 mM succinate/2 μM rotenone or 5 mM pyruvate/5 mM malate or 40 μM palmitoyl-L-carnitine/5 mM malate). By centrifugation at 2000 *g* for 20 minutes at 4°C mitochondria were attached to the plate bottom. Prewarmed (37°C) buffer containing substrate (180 μl per well, for substrates see above) were added after mitochondria were acclimatized for 5 minutes at RT. Finally, mitochondria were incubated for 30 minutes in the XF Prep Station at 37°C before the measurement of mitochondrial respiration was started.

Oxygen consumption was calculated by plotting oxygen concentration (nmol O_2) vs time (min). Mitochondrial respiration was measured in the presence of ADP and substrate (state 3), then 2.5 μg/μl oligomycin was injected to inhibit ATP-synthase (state 4o). Nonbiological background was assessed by addition of antimycin A (4 μM) and Rotenone (Rot, 2 μM) and subtracted from values of the other conditions. RCRs were calculated by dividing oxygen consumption during state 3 by oxygen consumption during state 4o respiration.

Measurement of mitochondrial membrane potential

Membrane potential (Ψ_m) of isolated mitochondria was measured by safranin O fluorescence (S884, Sigma-Aldrich; St. Louis, MO, USA). Measurements were conducted in a 96-well microplate (FLUOTRACTM 200, Greiner Bio-One, Frickenhausen, Germany) with 20 μg mitochondrial protein/well diluted in assay medium (KHE, 8 μM safranin O). Fluorescence signal intensity was recorded at an excitation of 495 nm and an emission wavelength of 586 nm at 37°C in a microplate reader (TECAN Infinite® M200, Tecan Group Ltd.). 15 kinetic cycles (à 1 minute) were measured before state 4 respiration was induced by either succinate/rotenone (5 mM/2 μM) or pyruvate/malate (5 mM). 10 further kinetic cycles were recorded until FCCP was injected to induce state 3u respiration. Measured fluorescence intensity was expressed as percentage of maximal fluorescence during state 3u (100%). $\Delta\Psi_m$ from state 4 to state 3u respiration was judged as ability of mitochondria to build up Ψ_m.

Immunoblotting

Immunoblots were performed with adipocyte protein lysates and isolated mitochondria, respectively. Proteins (adipocyte lysate: 37.5 μg; isolated mitochondria: 25 μg) were separated in a 12.5% SDS-PAGE and transferred to a nitrocellulose membrane (LI-COR® Biosciences; Lincoln, NE, USA, 60 minutes, 100V). Antibodies were targeted against citrate synthase (CS, 1:1000, Abcam, ab96600), COXIV (1:5000, Cell signaling, 4844), heat shock protein 60 (HSP60, 1:2000, Santa Cruz, sc-1052), histone H3 (1:2000, Cell signaling, 4499), OXPHOS (1:250, Mitosciences, MS604, just NDUFB and complex II- subunit 30 kDa were analyzable), superoxide dismutase 2 (SOD2, 1:10000, Abcam, ab16956) and voltage-dependent anion channel (VDAC, 1:900, Calbiochem, PC548). Infrared dye conjugated secondary antibodies (IRDye® 680, IRDye® 800, LI-COR®) were incubated at a dilution of 1:20000. The Odyssey software (LI-COR®) was applied to quantify band fluorescence intensities.

Measurement of mitochondrial superoxide

Superoxide release from isolated mitochondria was assessed indirectly as H_2O_2 using Amplex® Red fluorescence. Measurements were performed in a 96-well microplate (FLUOTRACTM 200, Greiner Bio-One) with 20 μg mitochondrial protein/well diluted in ROS medium (4 U/ml SOD, 2 U/ml HRP, 100 μM Amplex® Red). Signal intensity was recorded at an excitation of 560 nm and an emission wavelength of 590 nm at 37°C in a microplate reader (TECAN Infinite® M200, Tecan Group Ltd.). Ten kinetic cycles (à 1min) were measured before state 4 respiration was induced by 6 mM succinate/4 μM rotenone or 5 mM pyruvate/5 mM malate. 20 further kinetic cycles were measured. Superoxide production was also assessed during state 3 respiration (ADP). Absolute mitochondrial superoxide production translated in pmol H_2O_2/(min*mg mitochondrial protein) was calculated using a H_2O_2 standard.

Statistical Analyses

All data are presented as mean values ± standard deviation. For statistical comparison, Two-Way ANOVA followed by post hoc Bonferroni testing, Two-Way Repeated-Measures ANOVA followed by post hoc Bonferroni testing or two-tailed Student's t test were performed (SigmaPlot 12.5, Systat Software, Inc.; San Jose, CA, USA, GraphPad Prism4, GraphPad Software, Inc.; La Jolla, CA, USA). P values < 0.05 were considered statistically significant.

Results

Subcutaneous adipocytes display a higher respiratory capacity than visceral adipocytes

We compared the epididymal and the inguinal adipose tissue depots as representatives for murine visceral and subcutaneous fat. The total mass of these two anatomically distinct depots, and thus their relative contribution to total body fat mass, was comparable (inguinal WAT: 0.312 ± 0.061 g vs epididymal WAT: 0.291 ± 0.080 g, n = 89–90, $P < .001$). Cell size analysis revealed that adipocytes of inguinal origin are smaller than adipocytes of epididymal origin, as indicated by a smaller mean, median and 95th percentile diameter (figure S1). In random histological sections mean and median diameter seriously underestimate the real average cell size in both fat depots. Therefore, we chose the 95th percentile as the most realistic representation of cell diameter in the larger fraction of adipocytes (inguinal 42.9 μm, epididymal 56.4 μm).

We first assessed mitochondrial bioenergetics of intact white adipocytes to detect possible differences in oxidative function depending on anatomical localization. Respiration profiles were recorded by chamber based high-resolution respirometry (Oxygraph-2k, OROBOROS). Basal, leak and maximal cellular respiration rates were lower in epididymal when compared to inguinal adipocytes with the most significant difference for maximal respiration rate (figure 1A). Thus, the capacity for substrate oxidation is higher in inguinal adipocytes. We used absolute oxygen consumption rates to calculate key parameters of cellular respiratory control (31). Spare respiratory capacity (figure 1B) was higher in inguinal adipocytes, supporting a higher oxidative capacity of inguinal as compared to epididymal adipocytes. Thus, inguinal adipocytes are able to increase substrate oxidation to a higher extent in the case of a sudden increase in ATP demand.

In order to assess ADP dependent maximal oxidative phosphorylation (OXPHOS) capacity we conducted chamber based high-resolution respirometry of digitonin-permeabilized inguinal vs epididymal adipocytes (figure 2A). There was no difference in respiratory states determined by the proton leak (state 4 and state 4o) between both types of adipocytes. State 3 and state 3u respiration rates of inguinal adipocytes exceeded those from epididymal adipocytes, again showing a higher oxidative and respiratory capacity.

Notably, respiratory control ratios of inguinal and ep-

ididymal adipocytes were of comparable magnitude revealing tightly coupled mitochondria in adipocytes of both fat depots (figure 1C, 2B).

Taken together, inguinal adipocytes featured a markedly higher capacity for substrate turnover, reflected by both absolute respiration rates and spare respiratory capacity. Nonetheless, epididymal adipocytes were not dysfunctional per se as reflected by a high cRCR and RCR, respectively, which were both comparable to that of inguinal adipocytes.

Higher capacity for oxidative phosphorylation of inguinal adipocytes is attributable to higher mitochondrial capacity, not abundance

Principally, the observed difference in maximal respiratory capacity can be explained either by a different abundance of mitochondria in a cell or by a different capacity of the mitochondria themselves. To discriminate between these possibilities, we quantified several markers for mitochondrial abundance. Each of them, mtDNA content (figure 3A), citrate synthase activity level (figure 3B) and protein level of mitochondrial matrix proteins (citrate synthase, figure 3C; superoxide dismutase 2, figure 3D; heat shock protein 60, figure 3E) were comparable between adipocytes of both fat depots analyzed. Therefore, the differences observed in respirometry were not caused by differences in mitochondrial abundance per cell. To detect a possible difference in mitochondrial characteristics, we isolated mitochondria from inguinal and epididymal adipocytes and subjected them to plate based respirometry (XF96 Extracellular Flux Analyzer). As inguinal adipocytes are smaller when compared to epididymal adipocytes (figure S1), but contain equal amounts of mitochondria, isolation of mitochondria resulted in a higher yield per gram fat mass in inguinal vs epididymal fat cells (figure 3F). Respiring on all three different substrates succinate, pyruvate and palmitate, we consistently observed a higher capacity for oxidative phosphorylation (state 3) in mitochondria isolated from inguinal when compared to epididymal white adipocytes (figure 3G). Interestingly, we observed no differences in state 4o (proton leak dependent respiration) or respiratory control ratios indicating well coupled mitochondria in both types of adipocytes (figure 3H). Thus, the higher respiratory capacity of intact and permeabilized inguinal adipocytes is clearly attributable to a higher mitochondrial capability itself and does not result from a higher mitochondrial abundance.

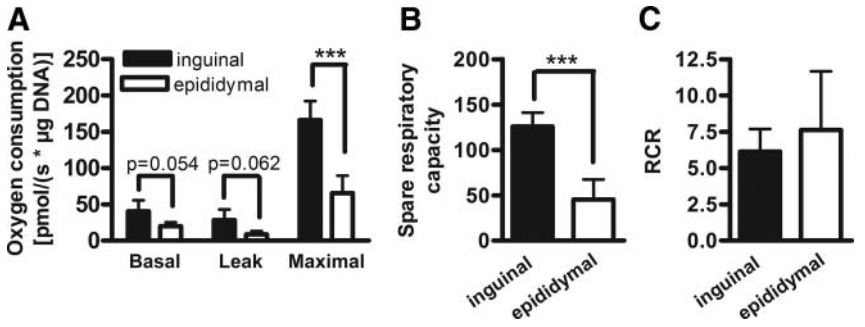

Figure 1. Cellular respiration of intact inguinal and epididymal adipocytes obtained by respiration analysis using the Oxygraph-2k. A, Higher respiratory capacity in inguinal adipocytes. After determination of basal respiration using pyruvate as substrate, we employed the ATP synthase inhibitor oligomycin to identify the proportion of basal respiration that contributes to either ATP turnover or proton leak, respectively. We added FCCP to determine the maximal cellular respiratory capacity. Finally, nonmitochondrial background was assessed by addition of complex III inhibitor antimycin A and subtracted from all other respiratory states. Oxygen consumption rates are expressed per μg DNA. *** = $P < .001$. **(B)** Higher spare respiratory capacity in inguinal adipocytes. Spare respiratory capacity was calculated by subtracting basal from maximal oxygen consumption rates. ***** =** $P < .001$. **(C)** No difference in mitochondrial integrity of inguinal and epididymal adipocytes. As indicator for mitochondrial integrity cellular respiratory control ratio (cRCR) was calculated as quotient of maximal to leak oxygen consumption. All data are presented as means ± SD of 8 independent experiments.

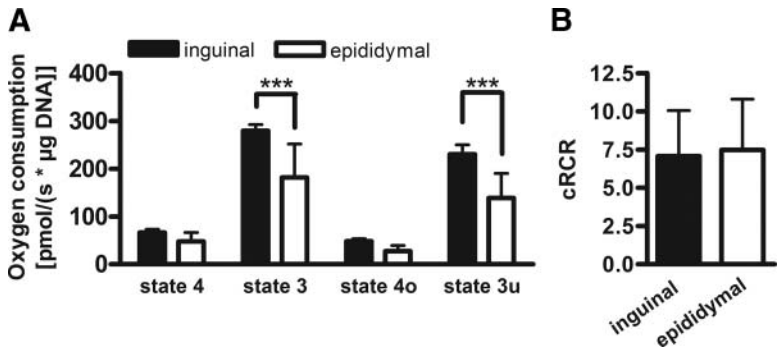

Figure 2. Oxygen consumption of permeabilized inguinal and epididymal adipocytes obtained by respiration analysis using the Oxygraph-2k. A, Higher oxidative and respiratory capacity in inguinal adipocytes. First, plasma membranes of adipocytes were permeabilized by digitonin and state 4 oxygen consumption was determined in the presence of succinate/rotenone before state 3 respiration was measured succeeded by addition of ADP. ATP-synthase was inhibited and state 4o respiration measured by addition of oligomycin. Next, state 3u was induced by addition of the uncoupler FCCP. Finally, injection of antimycin A led to blockade of electron flow and nonmitochondrial background was subtracted from other respiratory states. Oxygen consumption rates are expressed per μg DNA. *** = $P < .001$. **(B) No difference in mitochondrial integrity of permeabilized inguinal and epididymal adipocytes.** As indicator for mitochondrial integrity, mitochondrial respiratory control ratio (RCR) was calculated as ratio of state 3 to state 4o oxygen consumption. All data are presented as means ± SD of 8 independent experiments.

Furthermore, the capability of mitochondria to build up membrane potential (Ψ_m) was assessed using the membrane-permeant fluorescent dye safranin O. Independent of the substrate used (succinate/rotenone, figure 4A; pyruvate/malate, figure 4B), we observed a higher Ψ_m in inguinal when compared to epididymal adipocytes.

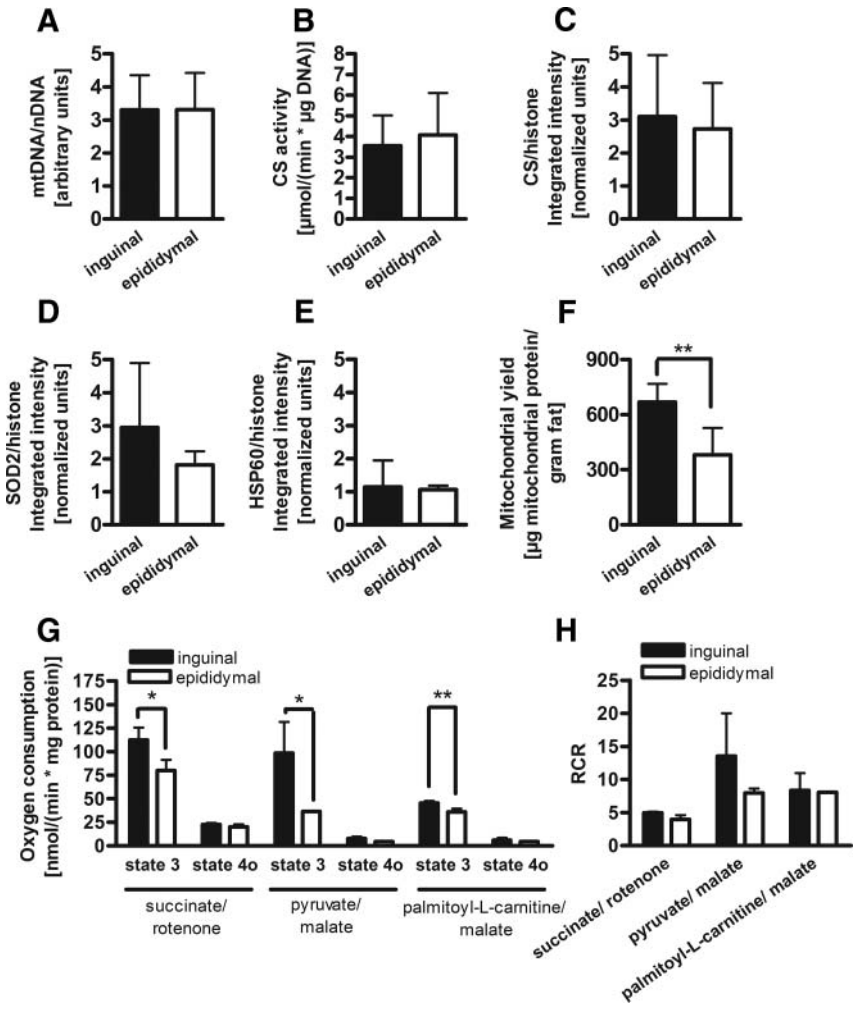

Figure 3. Higher capacity for oxidative phosphorylation of inguinal adipocytes is attributable to higher mitochondrial capacity, not abundance. **A,** Abundance of mtDNA (mtDNA) in adipocytes, relative to nuclear DNA (nDNA). Data are presented as means ± SD (n = 5). **(B)** Citrate synthase (CS) activity in adipocyte samples used for respiration analysis and normalized to the respective DNA content. Data are presented as means ± SD (n = 8). **(C-E)** Protein levels of mitochondrial citrate synthase (CS), superoxide dismutase 2 (SOD2), heat shock protein 60 (HSP60) determined by immunoblot analysis - normalized to histone H3. Data are presented as means ± SD (n = 3–4). **(F)** Mitochondrial yield from inguinal and epididymal white adipocytes. Data are presented as means ± SD (n = 6), ** = $P < .01$. **(G)** Bioenergetics of isolated white adipocyte mitochondria were measured using three different substrate combinations. First, phosphorylating state 3 respiration was assessed in the presence of ATP and substrate (succinate/rotenone, pyruvate/malate, palmitoyl-L-carnitine/malate). Then, ATP synthesis was inhibited and state 4o respiration was induced by oligomycin. Nonbiological background was determined by blockade of electron flow at complex III with antimycin A and subtracted from the other respiratory rates. Data are presented as mean values ± SD of 3 independent mitochondrial preparations. Two-Way Repeated-Measures ANOVA with Bonferroni posttest was performed for every substrate individually. * = $P < .05$. ** = $P < .01$. **(H)** No difference in mitochondrial integrity of mitochondria isolated from inguinal and epididymal adipocytes. As indicator for mitochondrial integrity respiratory control ratio (RCR) was calculated as ratio of state 3 to state 4o oxygen consumption. Data are presented as mean values ± SD of 3 independent mitochondrial preparations. Student's *t* test was performed for every substrate individually.

Higher mitochondrial respiratory capacity of inguinal adipocytes coincides with higher content in respiratory chain complexes

We further investigated the difference observed in oxidative phosphorylation of mitochondria isolated from inguinal and epididymal adipocytes by quantifying the protein amount of OXPHOS enzymes. We observed higher protein levels of complex I subunit NDUFB8, complex II-30 kDa subunit and complex IV subunit COX IV in mitochondria from inguinal vs epididymal adipocytes (figure 5A), independent of normalization to either mitochondrial outer membrane protein voltage-dependent anion channel (VDAC, depot effect $P < .01$) or matrix protein SOD2 (depot effect $P < .001$; figure 5B). No difference was observed relating VDAC to SOD2. Thus, the higher mitochondrial oxidative capacity of inguinal vs epididymal adipocytes can be ascribed to a more abundant respiratory chain per mitochondrion.

Taken together, all evidence supports a difference in maximal respiratory capacity specifically in the mitochondria of white inguinal and epididymal adipose tissue.

Higher superoxide production in relation to OXPHOS capacity in epididymal adipocytes

A high mitochondrial membrane potential can be associated with excessive production of reactive oxygen species (ROS) (32). We therefore determined ROS production in mitochondria isolated from both depots. In detail, we investigated whether mitochondria from inguinal and epididymal adipocytes differ in terms of superoxide radical anion (O_2^-) formation, the primary ROS generated by mitochondria. O_2^- is converted by superoxide dismutase 2 (SOD2) to membrane permeable H_2O_2 (33–35). For all tested conditions (state 3 and state 4 respiration of isolated mitochondria energized with succinate and pyruvate, respec-

tively) H_2O_2 release of mitochondria from inguinal and epididymal adipocytes was comparable (Table 1). Importantly, for pyruvate, the relative generation of O_2^- per nmol O_2 consumed at maximal OXPHOS performance was more than twice as high in mitochondria from epididymal vs inguinal adipocytes.

Short-time high-fat feeding impairs mitochondrial capacity mainly in epididymal adipocytes and affects body glucose homeostasis

To scrutinize whether the limitation in oxidative and respiratory capacity in epididymal vs inguinal adipocytes could account for the metabolic risk associated with visceral fat we exposed our mice to a metabolic challenge by feeding a high-fat diet (HFD) for one week. This experiment addressed the following hypotheses: i) the deficit in mitochondrial oxidative capacity of epididymal adipocytes could deteriorate during fat mass gain caused by HFD feeding and, ii) if white adipocyte mitochondrial dysfunction, particularly in visceral fat, is causally involved in the development of insulin resistance it must occur prior to or at least instantaneously with the emergence of impaired glucose metabolism.

In this feeding trial we determined the effect of a short-time HFD exposure on glucose metabolism and white adipocyte mitochondrial functionality comparing the two anatomically distinct fat depots. HFD feeding resulted in a slight but not significant increase in body weight and body fat content (figure 6A-B) as well as inguinal and epididymal fat pad mass (data not shown). Of note, HFD fed mice stood out by impaired glucose tolerance as indicated by a lower glucose clearance rate and a higher area under the curve (AUC) (AUC, figure 6 C, D).

Respirometry of intact adipocytes revealed markedly lowered maximal oxygen consumption in inguinal and epididymal adipocytes of the HFD group. No differences in basal and leak respiration were detected (figure 7A, B). Accordingly, spare respiratory capacity as the difference between maximal and basal respiration was lower in both types of adipocytes of HFD fed mice (figure 7C, D). From a comparable basal level, these adipocytes are unable to increase substrate oxidation in case of an increase in ATP demand to the same degree as adipocytes from CD fed mice do. CS activity as marker for mitochondrial abundance was lower in inguinal adipocytes of HFD fed mice but comparable in epididymal adipocytes (figure 7E, F). Cellular RCR was markedly lowered in epididymal but not inguinal adipocytes. Therefore, the difference in maximal respiratory capacity in inguinal adipocytes is most likely ascribable to a lowered mitochondrial abundance. Limited maximal cellular respiration and restricted spare respiratory capacity in epididymal adipocytes, however, was only ascribable to lowered mitochondrial capacity as indicated by comparable mitochondrial abundance but lowered cRCR.

Altogether, we here revealed that short-time HFD feeding affects mitochondrial capacity in white adipocytes. This functional limitation is much more pronounced in visceral-epididymal vs subcutaneous-inguinal adipocytes. As white adipocyte mitochondrial dysfunction, mainly in epididymal adipocytes, was paralleled by glucose intolerance a causal relationship is possible.

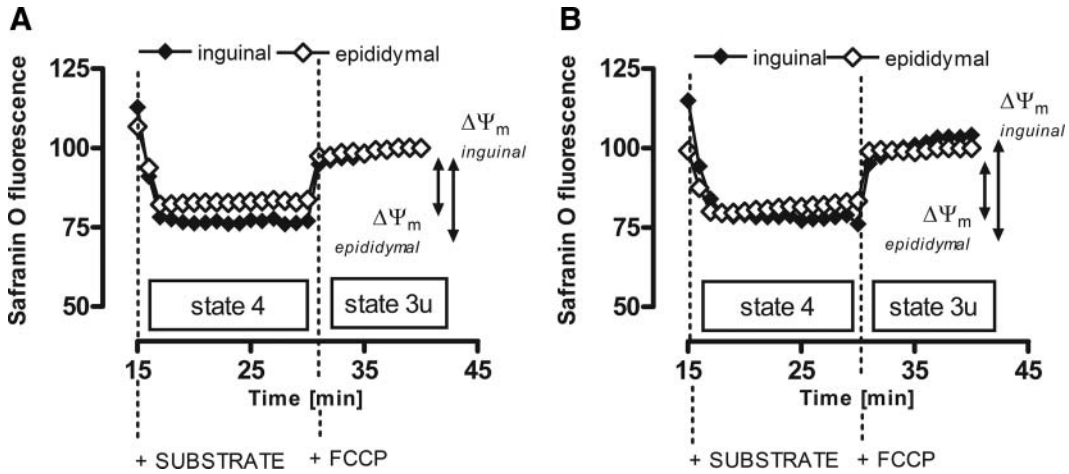

Figure 4. Isolated mitochondria from inguinal adipocytes show a higher potential (Ψ_m) across the mitochondrial inner membrane. Ψ_m was assessed by measuring safranin O fluorescence over 45 cycles (à 1 minute). The higher the potential across the mitochondrial inner membrane, the lower is the recorded fluorescence signal intensity. 15 minutes after starting the experiment, state 4 respiration was induced by injection of **(A)** succinate/rotenone or **(B)** pyruvate/malate. Finally, after 10 further minutes state 3u was induced by injection of the uncoupling agent FCCP. $\Delta\Psi_m$, from state 4 to state 3u respiration was judged as ability of mitochondria to build up Ψ_m. Data are presented as means of 3 independent experiments.

Table 1. Comparable H_2O_2 release rates in isolated mitochondria from inguinal and epididymal adipocytes

H_2O_2 release [pmol/(min*mg protein)]	succinate/rotenone		pyruvate/malate	
	state 3	**state 4**	**state 3**	**state 4**
inguinal	271 ± 97	349 ± 177	201 ± 77	218 ± 42
epididymal	200 ± 92	310 ± 150	158 ± 112	216 ± 56

H_2O_2 release was assessed in succinate (+ rotenone) or pyruvate/malate energized mitochondria isolated from inguinal and epididymal white adipocytes using Amplex Red fluorescence. Measurements were conducted during state 3 and state 4 respiration. Data are presented as means ± SD of 5–6 independent experiments.

Discussion

Alterations or differences in white adipocyte mitochondrial bioenergetics have repeatedly been implicated in the pathogenesis of insulin resistance and type 2 diabetes (36, 37). In addition, the mass of anatomically distinct fat depots exerts a divergent metabolic risk (4–7). In this study, we investigated whether this difference in risk coincides with a difference in mitochondrial function of white adipocytes.

We characterized mitochondrial bioenergetics of peripheral-inguinal and visceral-epididymal white adipocytes of lean and healthy, male C57Bl/6N mice by analyzing a comprehensive set of respiration parameters in cellular and organellar models. First, we isolated mature white adipocytes from inguinal and epididymal fat depots as the most physiological approach to assess cellular bioenergetics. Mitochondria are maintained in their undisturbed cellular environment and interactions with other cellular organelles or signaling molecules are preserved (31). Second, we determined maximal OXPHOS capacity by respirometry of digitonin-permeabilized adipocytes. Plasma membrane permeabilization still allows interaction of mitochondria with intracellular proteins, the cytoskeleton and intracellular membranes (38), hence conserving many aspects of normal cell physiology (31, 38). Notably, this approach bypasses the disadvantage of the permeability barrier given by the plasma membrane allowing ADP passage to induce maximal phosphorylating respiration. Third, we conducted respirometry of isolated white adipocyte mitochondria to analyze mitochondrial bioenergetics free from the influence of cellular factors and undisturbed by differences in mitochondrial abundance (39).

Adipocytes of inguinal white fat were characterized by a higher maximal respiratory capacity as compared to epididymal adipocytes. Leak (state 4o for isolated and permeabilized mitochondria) respiration rate was comparable between the two fat depots in all experimental setups. However, when mitochondria were brought to maximal oxygen consumption, either by chemical uncoupling or by addition of ADP, respiration of both epididymal adipocytes and their isolated mitochondria were consistently lower as compared to adipocytes and mitochondria of inguinal origin. This finding is in line with the lower abundance of respiratory complex I, II and IV in mitochondria of epididymal adipocytes. Since there is no difference detectable in states of low oxygen consumption, obviously epididymal adipocytes are more likely to attain at their bioenergetic limit in situations of high ATP demand.

In comparison, a higher mitochondrial abundance has been reported to cause a higher respiration of epididymal as compared to inguinal adipocytes in rats (40). Conversely, and in line with our findings, in obese humans subcutaneous adipose tissue displayed higher respiratory rates per cell and per mtDNA than visceral fat (41). Nonetheless,

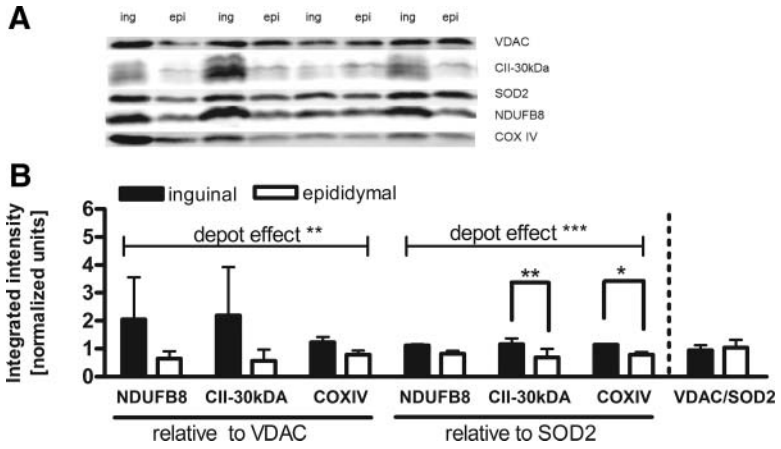

Figure 5. Mitochondria from inguinal adipocytes show higher protein levels of electron transport chain enzymes. A, Immunoblot of mitochondrial fractions isolated from inguinal (ing) and epididymal (epi) adipocytes against complex I subunit NDUFB, complex II-30 kDa subunit, complex IV subunit COXIV, outer membrane protein voltage-dependent anion channel (VDAC) and the matrix enzyme superoxide dismutase 2 (SOD2). B, NDUFB, CII-30 kDa and COX IV abundance in mitochondria normalized to VDAC and SOD2 and relation between matrix and outer membrane marker. Data are presented as means ± SD of 4 independent mitochondrial preparations. * = $P < .05$, ** = $P < .01$, *** = $P < .001$. Two-Way ANOVA with Bonferroni posttest was performed for VDAC and SOD2 individually.

as entire tissue biopsies were analyzed in that study, the contribution of the stromal vascular fraction to respiratory capacity remains elusive. Thus, to the best of our knowledge, the present study is the first demonstrating a higher metabolic capacity of subcutaneous adipocytes compared to visceral adipocytes due to higher mitochondrial performance.

Adipocyte heterogeneity in white adipose tissue depots may contribute to the observed differences in mitochondrial function. Brown-adipocyte like cells, known as *beige* or *brite* adipocytes, are inducible in subcutaneous fat, but are scarce in visceral fat (42, 43). In the induced state, these *brite* adipocytes contain more mitochondria than classical white adipocytes and express the thermogenic uncoupling protein 1 (44). In our study, however, the contribution of *brite* adipocytes seems negligible as adult C57Bl/6N mice housed at room temperature exhibit very low numbers of *brites* in white adipose tissue (45, 46). On the functional level, respiratory control ratios of mitochondria from inguinal and epididymal adipocytes were similar.

The main function of white adipose tissue is storage and mobilization of lipids. Lipogenesis, triglyceride synthesis and lipolysis are regulated dependent on organismic energy demand. In addition, white adipocytes exert various other functions including the synthesis and secretion of endocrine, paracrine and autocrine acting molecules known as adipokines which in concert contribute to the regulation of whole body metabolism (47). Each of these functions require functional, intact mitochondria with the ability to flexibly alter OXPHOS performance according to variable cellular ATP demand. Weight gain and obesity are metabolically challenging states for adipocytes, as for instance, triglyceride synthesis has to be increased due to the excessive fuel supply. As epididymal adipocytes are operating closer to their bioenergetic limit, they might fail to satisfy cellular ATP demands during this metabolic challenge before subcutaneous adipocytes do. Simultaneously, mitochondria from epididymal adipocytes generate higher levels of superoxide during maximal OXPHOS activity. This could interfere with cellular insulin signaling (48) or adipokine secretion (49, 50). In summary, a lower OXPHOS capacity combined with an increased ROS release in epididymal adipocytes can be regarded as metabolic inflexibility which further deteriorates during adipocyte hypertrophy. Possibly, this incapacity causes elevated oxidative damage, increased free fatty acid levels and an altered adipokine secretion pattern thereby contributing to the tremendous consequences of obesity for whole body energy and glucose homeostasis. Concordantly, visceral mass gain is a well-known risk factor for insulin resistance and type 2 diabetes (4–7) while expansion of subcutaneous adipose tissue even prevents the development of insulin resistance associated with obesity in laboratory mice (51). This is in line with our observation that HFD exposure for one week lowered white adipocyte mitochondrial capacity in adipocytes from visceral fat much more than in cells from inguinal fat, accompanied by the emergence of body glucose intolerance. A causal relationship between these two phenomena is possible.

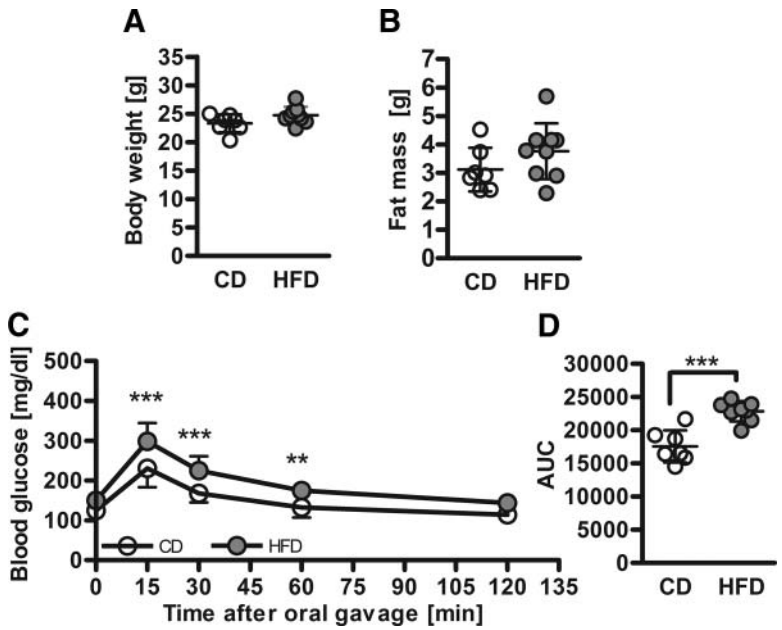

Figure 6. One week high-fat diet feeding causes impaired glucose tolerance. At the age of eight weeks mice were matched by body weight into a high-fat diet (HFD) and a control diet (CD) group. Diets were fed for one week. All parameters were measured at the end of the feeding period. **(A)** Body weight, **(B)** Fat mass, **(C)** Oral glucose tolerance test, **(D)** Total area-underthe-curve (AUC) calculated from C as measure for glucose tolerance. Data are presented as means ± SD (n = 7–9). ** = $P < .01$, *** = $P < .001$.

Taken together, we analyzed a suite of mitochondrial functions in intact and permeabilized cells and native organelles to reveal differences in mitochondrial bioenergetics of white adipocytes from anatomically distinct fat depots. The design of our study can serve as a starting point for further investigations focusing on comprehensive characterization of white adipocyte bioenergetics in the context of various metabolic diseases, dietary and genetic manipulations of body weight, pharmacological treatments, ageing and others.

Subcutaneous inguinal adipocytes displayed a markedly higher respiratory capacity and flexibility

when compared to mitochondria from epididymal fat. The divergent oxidative capacity was intrinsic to mitochondria and did not result from higher mitochondrial abundance or other intracellular structures and signals influencing mitochondrial function. Feeding a HFD for one week affected white adipocyte mitochondrial capacity, with much stronger deficits in epididymal when compared to inguinal adipocytes, paralleled by impaired whole body glucose homeostasis. The extent to which regional differences of adipose tissue depots in the vulnerability of their OXPHOS system accounts for the divergent metabolic risk of subcutaneous and visceral fat has to be clarified in future studies.

Acknowledgments

The Chair of Molecular Nutritional Medicine received financial support from by the Else Kröner-Fresenius Foundation (2007–2014). This study was partly funded by the Federal Ministry of Education and Research, Germany (BMBF AZ 0 315 674).

Address all correspondence and requests for reprints to: Dr. Martin Klingenspor, Professor for Molecular Nutritional Medicine, Technische Universität München, Gregor-Mendel-Str. 2, D-85 356 Freising-Weihenstephan, GERMANY, Phone +49 8161 71 2386, Fax +49 8161 71 2366, Email mk@tum.de

Disclosure: The authors have nothing to disclose

This work was supported by .

References

1. **Bjorndal Bodil BL, Staalesen Vidar, Skorve Jaon, Berge Rolf K.** Different Adipose Depots: Their Role in teh Development of Metabolic Syndrome and Mitochondrial Response to Hypolipidemic Agents. *Journal of obesity*. 2010.
2. **Kopelman PG.** Obesity as a medical problem. *Nature*. 2000; 404(6778):635–643.
3. **Kaur J.** A Comprehensive Review on Metabolic Syndrome. *Cardiology research and practice*. 2014;2014:943162.
4. **Vague J.** The degree of masculine differentiation of obesities: a factor determining predisposition to diabetes, atherosclerosis, gout, and uric calculous disease. *The American journal of clinical nutrition*. 1956;4(1):20–34.
5. **Bjorndal B, Burri L, Staalesen V, Skorve J, Berge RK.** Different adipose depots: their role in the development of metabolic syndrome and mitochondrial response to hypolipidemic agents. *Journal of obesity*. 2011;2011:490650.
6. **Tran TT, Yamamoto Y, Gesta S, Kahn CR.** Beneficial effects of subcutaneous fat transplantation on metabolism. *Cell metabolism*. 2008;7(5):410–420.
7. **Hocking SL, Chisholm DJ, James DE.** Studies of regional adipose transplantation reveal a unique and beneficial interaction between subcutaneous adipose tissue and the intra-abdominal compartment. *Diabetologia*. 2008;51(5): 900–902.
8. **Fox CS, Massaro JM, Hoffmann U, Pou KM, Maurovich-Horvat P, Liu CY, Vasan RS, Murabito JM, Meigs JB, Cupples LA, D'Agostino RB, Sr., O'Donnell CJ.** Abdominal visceral and subcutaneous adipose tissue compartments: association with metabolic risk factors in the Framingham Heart Study. *Circulation*. 2007;116(1):39–48.
9. **Lefebvre AM, Laville M, Vega N, Riou JP, van Gaal L, Auwerx J, Vidal H.** Depot-specific differences in adipose tissue gene expression in lean and obese subjects. *Diabetes*. 1998;47(1):98–103.
10. **Macotela Y, Emanuelli B, Mori MA, Gesta S, Schulz TJ, Tseng YH, Kahn CR.** Intrinsic differences in adipocyte precursor cells from different white fat depots. *Diabetes*. 2012;61(7):1691–1699.
11. **Sackmann-Sala L, Berryman DE, Munn**

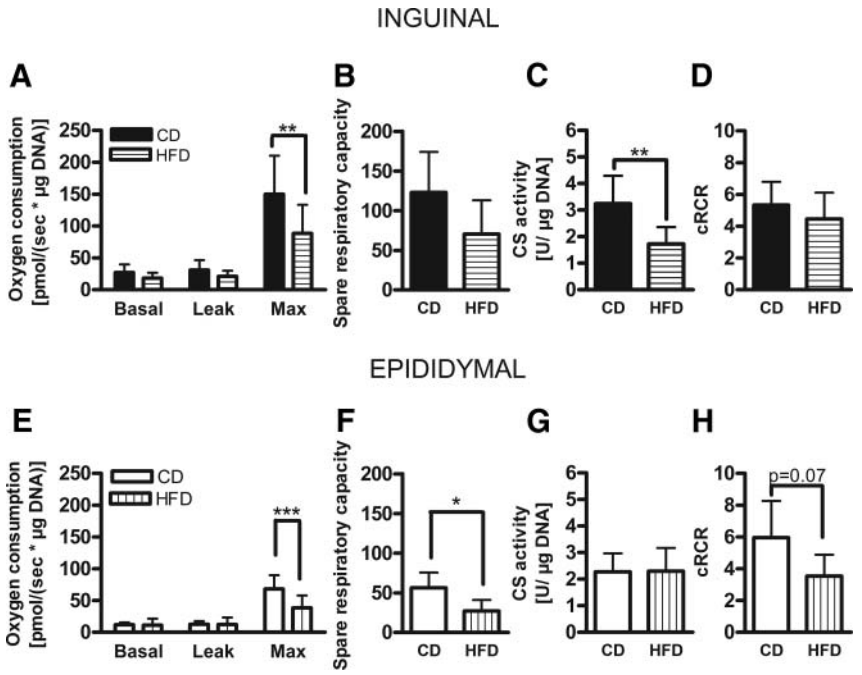

Figure 7. Cellular respiration of adipocytes from mice fed with high-fat diet (HFD) or control diet (CD) for one week obtained by respiration analysis using the Oxygraph-2k: HFD feeding results in limited maximal respiratory capacity in epididymal adipocytes. **(A, B)** After determination of basal respiration using pyruvate as substrate, we employed the ATP synthase inhibitor oligomycin to identify the proportion of basal respiration that contributes to either ATP turnover or proton leak, respectively. We added FCCP to determine the maximal cellular respiratory capacity. Finally, nonmitochondrial background was assessed by addition of complex III inhibitor antimycin A and subtracted from all other respiratory states. Oxygen consumption rates are expressed per μg DNA. **(C, D)** Lower Spare respiratory capacity in epiddymal adipocytes from HFD fed mice. Spare respiratory capacity = max – basal. **(E, F)** Lower mitochondrial abundance in inguinal adipocytes from HFD fed mice. Citrate synthase (CS) activity was measured as marker for mitochondrial abundance and expressed as CS activity per μg DNA. **(G, H)** Lower cellular respiratory control ratio (cRCR, quotient of maximal to leak oxygen consumption) in epididymal adipocytes of HFD fed mice. Data are presented as means ± SD (n = 6–8). * $P < .05$, ** = $P < .01$, *** = $P < .001$.

RD, Lubbers ER, Kopchick JJ. Heterogeneity among white adipose tissue depots in male C57BL/6J mice. *Obesity*. 2012; 20(1):101–111.

12. **Vohl MC, Sladek R, Robitaille J, Gurd S, Marceau P, Richard D, Hudson TJ, Tchernof A.** A survey of genes differentially expressed in subcutaneous and visceral adipose tissue in men. *Obesity research*. 2004;12(8):1217–1222.
13. **O'Rourke RW, Metcalf MD, White AE, Madala A, Winters BR, Maizlin, II, Jobe BA, Roberts CT, Jr., Slifka MK, Marks DL.** Depot-specific differences in inflammatory mediators and a role for NK cells and IFN-gamma in inflammation in human adipose tissue. *International journal of obesity*. 2009;33(9):978–990.
14. **Montague CT, O'Rahilly S.** The perils of portliness: causes and consequences of visceral adiposity. *Diabetes*. 2000;49(6):883–888.
15. **Hellmer J, Marcus C, Sonnenfeld T, Arner P.** Mechanisms for differences in lipolysis between human subcutaneous and omental fat cells. *The Journal of clinical endocrinology and metabolism*. 1992; 75(1):15–20.
16. **Richelsen B, Pedersen SB, Moller-Pedersen T, Bak JF.** Regional differences in triglyceride breakdown in human adipose tissue: effects of catecholamines, insulin, and prostaglandin E2. *Metabolism: clinical and experimental*. 1991;40(9):990–996.
17. **Alessi MC, Peiretti F, Morange P, Henry M, Nalbone G, Juhan-Vague I.** Production of plasminogen activator inhibitor 1 by human adipose tissue: possible link between visceral fat accumulation and vascular disease. *Diabetes*. 1997;46(5):860–867.
18. **Fried SK, Bunkin DA, Greenberg AS.** Omental and subcutaneous adipose tissues of obese subjects release interleukin-6: depot difference and regulation by glucocorticoid. *The Journal of clinical endocrinology and metabolism*. 1998;83(3):847–850.
19. **Montague CT, Prins JB, Sanders L, Digby JE, O'Rahilly S.** Depot- and sex-specific differences in human leptin mRNA expression: implications for the control of regional fat distribution. *Diabetes*. 1997;46(3):342–347.
20. **Chau YY, Bandiera R, Serrels A, Martinez-Estrada OM, Qing W, Lee M, Slight J, Thornburn A, Berry R, McHaffie S, Stimson RH, Walker BR, Chapuli RM, Schedl A, Hastie N.** Visceral and subcutaneous fat have different origins and evidence supports a mesothelial source. *Nature cell biology*. 2014;16(4):367–375.
21. **Giordano A, Smorlesi A, Frontini A, Barbatelli G, Cinti S.** White, brown and pink adipocytes: the extraordinary plasticity of the adipose organ. *European journal of endocrinology / European Federation of Endocrine Societies*. 2014;170(5):R159–171.
22. **Cinti S.** The adipose organ. *Prostaglandins, leukotrienes, and essential fatty acids*. 2005;73(1):9–15.
23. **Frontini A, Cinti S.** Distribution and development of brown adipocytes in the murine and human adipose organ. *Cell metabolism*. 2010;11(4):253–256.
24. **Rong JX, Qiu Y, Hansen MK, Zhu L, Zhang V, Xie M, Okamoto Y, Mattie MD, Higashiyama H, Asano S, Strum JC, Ryan TE.** Adipose mitochondrial biogenesis is suppressed in db/db and high-fat diet-fed mice and improved by rosiglitazone. *Diabetes*. 2007;56(7): 1751–1760.
25. **Wang PW, Kuo HM, Huang HT, Chang AY, Weng SW, Tai MH, Chuang JH, Chen IY, Huang SC, Lin TK, Liou CW.** Biphasic Response of Mitochondrial Biogenesis to Oxidative Stress in Visceral Fat of Diet-Induced Obesity Mice. *Antioxidants, redox signaling*. 2014.
26. **Dahlman I, Forsgren M, Sjogren A, Nordstrom EA, Kaaman M, Naslund E, Attersand A, Arner P.** Downregulation of electron transport chain genes in visceral adipose tissue in type 2 diabetes independent of obesity and possibly involving tumor necrosis factor-alpha. *Diabetes*. 2006;55(6):1792–1799.
27. **Choo HJ, Kim JH, Kwon OB, Lee CS, Mun JY, Han SS, Yoon YS, Yoon G, Choi KM, Ko YG.** Mitochondria are impaired in the adipocytes of type 2 diabetic mice. *Diabetologia*. 2006;49(4):784–791.
28. **Bogacka I, Xie H, Bray GA, Smith SR.** Pioglitazone induces mitochondrial biogenesis in human subcutaneous adipose tissue in vivo. *Diabetes*. 2005;54(5):1392–1399.
29. **Lindinger A, Peterli R, Peters T, Kern B, von Flue M, Calame M, Hoch M, Eberle AN, Lindinger PW.** Mitochondrial DNA content in human omental adipose tissue. *Obesity surgery*. 2010;20(1):84–92.
30. **Even PC, Nadkarni NA.** Indirect calorimetry in laboratory mice and rats: principles, practical considerations, interpretation and perspectives. *American journal of physiology Regulatory, integrative and comparative physiology*. 2012;303(5):R459–476.
31. **Brand MD, Nicholls DG.** Assessing mitochondrial dysfunction in cells. *The Biochemical journal*. 2011;435(2):297–312.
32. **Korshunov SS, Skulachev VP, Starkov AA.** High protonic potential actuates a mechanism of production of reactive oxygen species in mitochondria. *FEBS letters*. 1997;416(1):15–18.
33. **Loschen G, Azzi A.** On the formation of hydrogen peroxide and oxygen radicals in heart mitochondria. *Recent advances in studies on cardiac structure and metabolism*. 1975;7:3–12.
34. **Loschen G, Azzi A, Richter C, Flohe L.** Superoxide radicals as precursors of mitochondrial hydrogen peroxide. *FEBS letters*. 1974; 42(1):68–72.
35. **Boveris A, Cadenas E.** Mitochondrial production of superoxide anions and its relationship to the antimycin insensitive respiration. *FEBS letters*. 1975;54(3):311–314.
36. **Kusminski CM, Holland WL, Sun K, Park J, Spurgin SB, Lin Y, Askew GR, Simcox JA, McClain DA, Li C, Scherer PE.** MitoNEET-driven alterations in adipocyte mitochondrial activity reveal a crucial adaptive process that preserves insulin sensitivity in obesity. *Nature medicine*. 2012;18(10):1539–1549.
37. **Vernochet C, Mourier A, Bezy O, Macotela Y, Boucher J, Rardin MJ, An D, Lee KY, Ilkayeva OR, Zingaretti CM, Emanuelli B, Smyth G, Cinti S, Newgard CB, Gibson BW, Larsson NG, Kahn CR.** Adipose-specific deletion of TFAM increases mitochondrial oxidation and protects mice against obesity and insulin resistance. *Cell metabolism*. 2012;16(6):765–776.
38. **Appaix F, Kuznetsov AV, Usson Y, Kay L, Andrienko T, Olivares J, Kaambre T, Sikk P, Margreiter R, Saks V.** Possible role of cytoskeleton in intracellular arrangement and regulation of mitochondria. *Experimental physiology*. 2003;88(1):175–190.
39. **Perry CG, Kane DA, Lanza IR, Neufer PD.** Methods for assessing mitochondrial function in diabetes. *Diabetes*. 2013;62(4):1041–1053.
40. **Deveaud C, Beauvoit B, Salin B, Schaeffer J, Rigoulet M.** Regional differences in oxidative capacity of rat white adipose tissue are linked to the mitochondrial content of mature adipocytes. *Molecular and cellular biochemistry*. 2004;267(1–2):157–166.
41. **Kraunsoe R, Boushel R, Hansen CN, Schjerling P, Qvortrup K, Stockel M, Mikines KJ, Dela F.** Mitochondrial respiration in subcutaneous and visceral adipose tissue from patients with morbid obesity. *The Journal of physiology*. 2010;588(Pt 12):2023–2032.
42. **Barbatelli G, Murano I, Madsen L, Hao Q, Jimenez M, Kristiansen K, Giacobino JP, De Matteis R, Cinti S.** The emergence of cold-induced brown adipocytes in mouse white fat depots is determined predominantly by white to brown adipocyte transdifferentiation. *American journal of physiology Endocrinology and metabolism*. 2010;298(6):E1244–1253.
43. **Guerra C, Koza RA, Yamashita H, Walsh K, Kozak LP.** Emergence of brown adipocytes in white fat in mice is under genetic control. Effects on body weight and adiposity. *The Journal of clinical investigation*. 1998;102(2):412–420.
44. **Li Y, Lasar D, Fromme T, Klingenspor M.** White, brite, and brown adipocytes: the evolution and function of a heater organ in mammals. *Canadian Journal of Zoology*. 2014;92:615–626.
45. **Xue B, Coulter A, Rim JS, Koza RA, Kozak LP.** Transcriptional synergy and the regulation of Ucp1 during brown adipocyte induction in white fat depots. *Molecular and cellular biology*. 2005; 25(18):8311–8322.

46. **Okamatsu-Ogura Y, Fukano K, Tsubota A, Uozumi A, Terao A, Kimura K, Saito M.** Thermogenic ability of uncoupling protein 1 in beige adipocytes in mice. *PloS one*. 2013;8(12):e84229.
47. **Lago F, Dieguez C, Gomez-Reino J, Gualillo O.** Adipokines as emerging mediators of immune response and inflammation. *Nature clinical practice Rheumatology*. 2007;3(12):716–724.
48. **Lin Y, Berg AH, Iyengar P, Lam TK, Giacca A, Combs TP, Rajala MW, Du X, Rollman B, Li W, Hawkins M, Barzilai N, Rhodes CJ, Fantus IG, Brownlee M, Scherer PE.** The hyperglycemia-induced inflammatory response in adipocytes: the role of reactive oxygen species. *The Journal of biological chemistry*. 2005;280(6):4617–4626.
49. **Soares AF, Guichardant M, Cozzone D, Bernoud-Hubac N, Bouzaidi-Tiali N, Lagarde M, Geloen A.** Effects of oxidative stress on adiponectin secretion and lactate production in 3T3–L1 adipocytes. *Free radical biology, medicine*. 2005;38(7):882–889.
50. **Furukawa S, Fujita T, Shimabukuro M, Iwaki M, Yamada Y, Nakajima Y, Nakayama O, Makishima M, Matsuda M, Shimomura I.** Increased oxidative stress in obesity and its impact on metabolic syndrome. *The Journal of clinical investigation*. 2004;114(12):1752–1761.
51. **Kim JY, van de Wall E, Laplante M, Azzara A, Trujillo ME, Hofmann SM, Schraw T, Durand JL, Li H, Li G, Jelicks LA, Mehler MF, Hui DY, Deshaies Y, Shulman GI, Schwartz GJ, Scherer PE.** Obesity-associated improvements in metabolic profile through expansion of adipose tissue. *The Journal of clinical investigation*. 2007;117(9):2621–2637.